Cardiac neural crest of the mouse embryo: axial level of origin, migratory pathway and cell autonomy of the *splotch* (*Sp^{2H}*) mutant effect

Wood Yee Chan[1,*], Chui Shan Cheung[1], Kim Ming Yung[1] and Andrew J. Copp[2]

[1]Department of Anatomy, Faculty of Medicine, The Chinese University of Hong Kong, Hong Kong, China
[2]Neural Development Unit, Institute of Child Health, University College London, London WC1N 1EH, UK
*Author for correspondence (e-mail: wy-chan@cuhk.edu.hk)

Accepted 24 March 2004

Development 131, 3367-3379
Published by The Company of Biologists 2004
doi:10.1242/dev.01197

Summary

A sub-population of the neural crest is known to play a crucial role in development of the cardiac outflow tract. Studies in avians have mapped the complete migratory pathways taken by 'cardiac' neural crest cells en route from the neural tube to the developing heart. A cardiac neural crest lineage is also known to exist in mammals, although detailed information on its axial level of origin and migratory pattern are lacking. We used focal cell labelling and orthotopic grafting, followed by whole embryo culture, to determine the spatio-temporal migratory pattern of cardiac neural crest in mouse embryos. Axial levels between the post-otic hindbrain and somite 4 contributed neural crest cells to the heart, with the neural tube opposite somite 2 being the most prolific source. Emigration of cardiac neural crest from the neural tube began at the 7-somite stage, with cells migrating in pathways dorsolateral to the somite, medial to the somite, and between somites. Subsequently, cardiac neural crest cells migrated through the peri-aortic mesenchyme, lateral to the pharynx, through pharyngeal arches 3, 4 and 6, and into the aortic sac. Colonisation of the outflow tract mesenchyme was detected at the 32-somite stage. Embryos homozygous for the *Sp^{2H}* mutation show delayed onset of cardiac neural crest emigration, although the pathways of subsequent migration resembled wild type. The number of neural crest cells along the cardiac migratory pathway was significantly reduced in *Sp^{2H}/Sp^{2H}* embryos. To resolve current controversy over the cell autonomy of the *splotch* cardiac neural crest defect, we performed reciprocal grafts of premigratory neural crest between wild type and *splotch* embryos. *Sp^{2H}/Sp^{2H}* cells migrated normally in the +/+ environment, and +/+ cells migrated normally in the *Sp^{2H}/Sp^{2H}* environment. In contrast, retarded migration along the cardiac route occurred when either *Sp^{2H}*/+ or *Sp^{2H}/Sp^{2H}* neural crest cells were grafted into the *Sp^{2H}/Sp^{2H}* environment. We conclude that the retardation of cardiac neural crest migration in *splotch* mutant embryos requires the genetic defect in both neural crest cells and their migratory environment.

Key words: Cardiac neural crest, Migration, *splotch*, Labelling, Transplantation, Embryo culture, WGA-Au, DiI, Grafting, Outflow tract, Persistent truncus arteriosus

Introduction

The cardiac neural crest is a migratory cell population that emerges from the occipital region of the neural tube and migrates through the cranial mesenchyme to the aortic sac and the cardiac outflow tract (Kirby et al., 1983; Kirby and Waldo, 1995). Neural crest cells are crucial for cardiovascular development, forming the neurons and supporting cells of the cardiac ganglia (Verberne et al., 1998; Kirby and Stewart, 1983), and participating in the formation of the aorto-pulmonary septum that divides the outflow tract into ascending aorta and pulmonary trunk (Kirby et al., 1983; Conway et al., 1997; Conway et al., 2000; Jiang et al., 2000; Epstein et al., 2000). Ablation of the premigratory cardiac neural crest in avian embryos results in malformations of the outflow tract, including persistent truncus arteriosus, interruption of the aortic arch and double outlet right ventricle (Kirby et al., 1983).

In mammals, a role for the cardiac neural crest during cardiovascular development has been established through studies of several mouse mutants with congenital heart defects that affect the outflow tract and great vessels (Esptein, 1996; Conway et al., 1997; Yanagisawa et al., 1998; Brannan et al., 1994; Lo et al., 1999; Winnier et al., 1999). Moreover, neural crest defects have been implicated in the pathogenesis of some forms of human congenital heart disease including DiGeorge/velocardiofacial syndrome (Lipson et al., 1991; Driscoll, 1994) and retinoic acid embryopathy (Rothman et al., 1995).

The majority of information on neural crest migration has been derived from chick embryos using quail-to-chick chimaeras, in situ cell labelling, immunohistochemistry and ablation of the premigratory neural crest (Le Douarin and Kalcheim, 1999). In mammals, the lack of morphological features or specific markers that allow neural crest cells to be identified throughout the majority of their developmental time course has hampered the investigation of their migration and

differentiative fate. Exogenous cell labelling in rodents has provided information on the migratory pathways of the neural crest to the heart (Fukiishi and Morriss-Kay, 1992; Osumi-Yamashita et al., 1996). Moreover, several molecular markers, both intrinsic (Conway et al., 1997) and transgenic (Lo et al., 1997; Liu et al., 1994; Means and Gudas, 1997; Serbedzija and McMahon, 1997), have also been used to trace the initial migratory population of the cardiac neural crest. Definitive evidence for a contribution of the mammalian neural crest to cardiovascular development was provided by fate-mapping studies in the mouse using a transgenic system based on Cre/loxP recombination (Jiang et al., 2000). The conclusion from these studies is that the mammalian cardiac neural crest arises from the occipital region of the neural tube and populates the outflow tract similarly to avians.

Despite these several previous studies, several unanswered questions remain concerning the mammalian cardiac neural crest. First, the specific rostrocaudal level of origin of the cardiac neural crest lineage has not been determined. Second, there has been no detailed spatio-temporal study of the route taken by the mammalian neural crest en route to the heart. Third, considerable controversy surrounds the issue of the cell-autonomy or non-cell-autonomy of the neural crest defects in the *splotch* mutant mouse, a much-studied mammalian genetic model of abnormal cardiac neural crest development (Auerbach, 1954; Franz, 1989; Epstein, 1996). In the present study, we have investigated these three questions using an experimental design involving exogenous labelling of mouse cardiac neural crest, followed by whole embryo culture in order to trace neural crest cell migration in the intact embryo. We used two cell labels, wheat germ agglutinin gold conjugates (WGA-Au) (Smits-van Prooije et al., 1986; Chan and Tam, 1988; Trainor and Tam, 1995) and DiI, to label the premigratory neural crest by direct microinjection or by orthotopic transplantation of a fragment of labelled neural crest tissue into an unlabelled embryo. In addition, we followed neural crest migration in the *splotch* (Sp^{2H}) mouse mutant and performed reciprocal neural crest transplants between embryos of different genotypes to determine the degree of cell autonomy of the *splotch* neural crest migration defect.

Materials and methods

Preparation of WGA-Au and DiI

WGA-Au and DiI labelling solutions were prepared as described by Chan and Tam (Chan and Tam, 1988) and Serbedzija et al. (Serbedzija et al., 1992), respectively. Briefly, WGA lectin (Sigma) was first cross-linked to bovine serum albumin (BSA, Sigma) in 0.25% glutaraldehyde. WGA-BSA complexes were then conjugated with colloid gold particles (0.005% of 15-25 nm particles in citrate buffer, pH 5.0; Polysciences, Warrington, PA, USA) in 10% M-20 polyethylene glycol (Sigma). The solution was adjusted to pH 7.0 by 0.1 M KCl and was spun at 120,000 ***g*** at 4°C. A deep red WGA-Au solution was obtained by suspending the pellet in 50 μl of the original buffer. DiI (1,1′-dioctadecyl-3,3,3′,3′-tetramethyl indocarbocyanine perchlorate, Molecular Probes) was prepared by dissolving 5 mg crystals in 1 ml absolute ethanol. After centrifugation at 13,600 ***g*** for 10 minutes, 100 μl of the solution was diluted with 1 ml of 0.3 M sucrose solution.

Mouse strains and embryo isolation

Random bred ICR (Institute of Cancer Research, Harlan, Oxfordshire, UK) mice were used for studies of normal neural crest migration. Random bred *splotch* (Sp^{2H}) mice, which harbour an intragenic deletion of the *Pax3* gene, were genotyped as described previously (Epstein et al., 1991). Both mouse strains were kept under a 12-hour light:12-hour dark cycle at the Laboratory Animal Services Centre of The Chinese University of Hong Kong. Noon on the day of finding a copulation plug was designated E0.5 assuming that copulation occurred around midnight. Pregnant mice were sacrificed by cervical dislocation at E8.0 to E8.5, and embryos at various somite stages were dissected from the decidua in PB1 medium (Whittingham and Wales, 1969). The visceral yolk sac and ectoplacental cone were kept intact while Reichert's membrane and its adherent parietal endodermal cells were removed (Chan and Tam, 1988; Chan and Lee, 1992).

In situ focal labelling

DiI or WGA-Au solution was directly deposited in the vicinity of the neural crest by microinjection using a Leitz micromanipulator on a Wild stereomicroscope (Chan and Tam, 1988; Chan et al., 2003). Injection pipettes were prepared from glass micropipettes of internal diameter 0.85 mm (GC100T-15, Clark Electromedical Instruments, Kent, UK) using a vertical pipette puller (KOPF Instruments, Model 720, Tujunga, CA, USA) to give an internal diameter of approximately 10-15 μm. The tip of the injection pipette was heat-polished with a microforge (Narishige Scientific, MF-79, Setagaya-ku, Tokyo, Japan). The deep red WGA-Au solution or the slightly reddish-yellow DiI solution was slowly dispensed from the injection pipette, under the control of an oil pump (DeFonbrune, CIT-ALCATEL, Paris, France), onto the dorsal margins of the neuroepithelium at different axial levels of the hindbrain (Fig. 1A) after the injection pipette pierced through the visceral yolk sac and the amnion. At the level of somites 4 and 5, where the neural tube was already closed, the injection pipette punctured the surface epithelium to label the dorsal neural tube. Care was taken not to spill the labelling solution onto the surface epithelium, so as to avoid labelling the epibranchial placodes, which are known to contribute migrating cells within the cranial mesenchyme (Lumsden et al., 1991; Le Douarin and Kalcheim, 1999). The injection site was checked carefully after injection. If the labelled neural crest region was found to extend over a rostrocaudal distance of more than one somite length, or if the labelling site did not correspond to the intended region, the embryo was discarded from further analysis.

Microsurgical grafting of neural crest fragments

Orthotopic grafting was performed in mouse embryos with 5 to 6 somites as described by Chan and Tam (Chan and Tam, 1988) with modifications. The embryonic region rostral to the upper margin of the forelimb bud was excised and incubated in PB1 containing 0.5 mg/ml dispase (Gibco) for 8 to 10 minutes at room temperature. Neural tube or neural plate was then dissected free of the adjacent mesenchyme and surface epithelium, incubated in WGA-Au for 5 minutes or in DiI for 1 minute, and washed with several changes of PB1. Then, donor neural crest fragments of 30 to 50 cells were isolated with fine tungsten needles from the neural plate/tube at the level of prorhombomere b (ProRhB; forerunner of rhombomeres 3 and 4) (Osumi-Yamashita et al., 1996), prorhombomere c (ProRhC; forerunner of rhombomeres 5 and 6) or somites 1 to 4 (Fig. 1A). Grafting was performed with a micromanipulator, using pipettes (internal diameter 20 μm) prepared as described above. The pipette, loaded with a neural crest fragment, was pushed through the visceral yolk sac and amnion and advanced until the dorsal surface of the host embryo was penetrated at the neural crest region. As the pipette was slowly withdrawn, the fragment was released into the graft site with the aid of the DeFonbrune oil pump. After grafting, the exact position of the graft, which was labelled red with WGA-Au or yellow with DiI, was immediately checked. Only embryos in which a graft had been properly placed were used for embryo culture.

Embryo culture

Embryos after labelling or grafting were cultured in groups of five in 50 ml serum bottles containing 5 ml of heat-inactivated (56°C for 30 minutes), immediately centrifuged pure rat serum. The cultures were kept in a roller system at 37°C for a maximum of 48 hours (Chan and Tam, 1988; Chan and Lee, 1992). Assessment of mean somite number, mean crown-rump length and a series of morphological features revealed no significant differences between E8.5 non-mutant ICR embryos developing in culture for 48 hours and E8.5 control embryos developing entirely in vivo (data not shown). Moreover, focal labelling and orthotopic grafting had no significant effect on the success of embryonic development in culture. E8.5 embryos from *splotch* litters, whether focally labelled, grafted or unoperated, grew and developed in culture with no significant differences from ICR embryos (data not shown).

Processing of cultured embryos

Embryos that had been labelled with WGA-Au or grafted with a WGA-Au-labelled fragment were dissected free of extraembryonic membranes, rinsed in PBS, fixed in Carnoy's fixative for 45 minutes and processed for paraffin wax histology. Serial transverse sections of 6 μm thickness were prepared through the hindbrain region and stained with silver (Chan and Lee, 1992). Embryos labelled with DiI were rinsed in PBS, fixed in 4% paraformaldehyde for 18 to 20 hours and dehydrated in a graded series (10-30%) of sucrose solutions before embedding in OCT compound (Tissue-TEK). Serial transverse sections were cut at 16 μm on a cryostat (Shandon, Cheshire, UK) and examined under a Zeiss epifluorescence microscope equipped with a rhodamine filter.

Cell counting

Following WGA-Au focal injection, labelled neural crest cells with silver granules in their cytoplasm were counted only in sections in which more than 90% of the cells of the dorsal part of the neural tube were silver granule-laden. This ensured that only fully labelled embryos were analysed in detail. Cell counts were performed at 400× magnification on a Zeiss Axioplan2 microscope linked to a Spot-Cooled Color Digital Camera (Diagnostic Instruments, Sterling Heights, MI, USA). Images were captured with a MetaMorph Imaging System (Universal Imaging Corporation, Downington, PA, USA). The number of labelled cells at each time point was computed from at least five embryos. The regions where cell counting was performed were defined as: (1) trigeminal and facio-acoustic ganglia: discrete aggregates of cells in the cranial mesenchyme; (2) second pharyngeal arches: all labelled cells beneath the pharyngeal arch epithelium; (3) medial neural crest migratory pathway: labelled cells within the mesenchymal region between neural tube and somite extending dorsoventrally from the dorsal edge of the somite to its ventral tip; (4) peri-aortic mesenchyme: the circular area surrounding the dorsal aorta with a width equal to the radius of the vessel; (5) mesenchymal region lateral to the pharynx: all cells between the dorsoventral extent of the pharynx and the surface epithelium.

Statistical analysis

Morphological scores were compared by Chi-squared test whereas somite numbers, crown-rump lengths and cell numbers were compared by unrelated Student's two-tailed *t*-test. The level of significance was set at $P<0.05$.

Results

Axial level of origin of the mouse cardiac neural crest

To determine which axial levels contribute neural crest cells to the mouse cardiac outflow tract, the neural crest regions at ProRhB, ProRhC or at the axial levels of somites 1, 2, 3, 4 or 5 (S1, S2, S3, S4 or S5) were individually labelled with DiI, or grafted with a DiI-labelled neural crest fragment (Fig. 1A). A total of 119 non-mutant ICR embryos were successfully labelled with DiI and most (93%) developed normally in vitro. Of the 68 embryos grafted with a labelled neural crest fragment, 51 (75%) had a graft in the intended region (Fig. 1B) and these were subsequently cultured. Most (92%) of these grafted embryos underwent normal development in vitro for 48 hours and were analysed further. In some embryos, labelled cells remained associated with the graft site after the culture period (Fig. 1C).

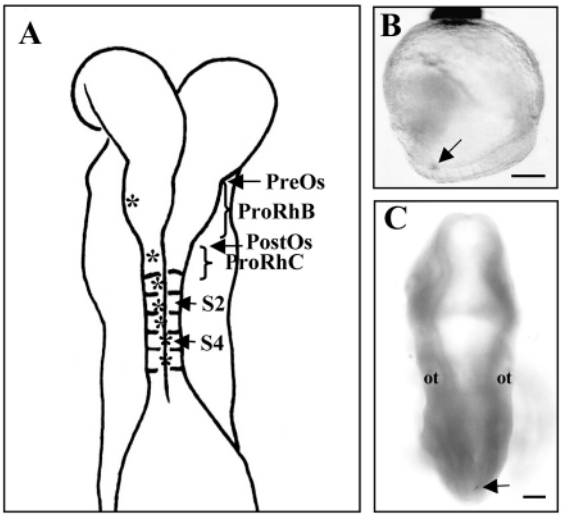

Fig. 1. (A) Drawing of the dorsal view of an E8.5 Institute of Cancer Research (ICR) mouse embryo with 5 somites. Labelling/graft sites (*) were located on the left side of the embryo at the lateral margin of the neural plate, where the neural tube had not yet completely closed [prorhombomere b (ProRhB), prorhombomere c (ProRhC) and at levels of somites 1-3], or in the dorsal part of the closed neural tube [at levels of somites 4 (S4) and 5 (S5)]. The neural crest of ProRhB was injected or grafted just rostral to the position of the otic placode. The definition of prorhombomeres follows Osumi-Yamashita et al. (Osumi-Yamashita et al., 1996). PreOs, preotic sulcus; PostOs, postotic sulcus. (B) Lateral view of an E8.5 ICR embryo immediately following grafting with a DiI-labelled neural crest fragment (arrow). (C) Dorsal view of an embryo 48 hours following grafting. The graft site is indicated by the arrow. Scale bars: 250 μm in B; 160 μm in C. ot, otic vesicle.

When ProRhB was labelled (Fig. 2A), a stream of labelled cells was observed to traverse the cranial mesenchyme to the second pharyngeal arch (Fig. 2B). No labelled cells were found in the cardiac outflow tract (Fig. 3) or any other cardiac structures. When the labelling site was ProRhC, labelled cells were distributed along a subepithelial pathway to the third pharyngeal arches (Fig. 2C,D). This pathway extended dorsoventrally from the neural crest to the vicinity of the developing pharynx (Fig. 2D). A similar distribution of labelled cells was found when a DiI-labelled neural crest fragment was grafted orthotopically to ProRhC (Fig. 2E,F). Of the 41 embryos labelled or grafted at the level of ProRhC, only three (7.3%) showed labelled cells in the cardiac outflow tract (Fig. 3), indicating that the neural crest from ProRhC is not a major source of cardiac neural crest.

When the labelling or grafting was performed at somitic

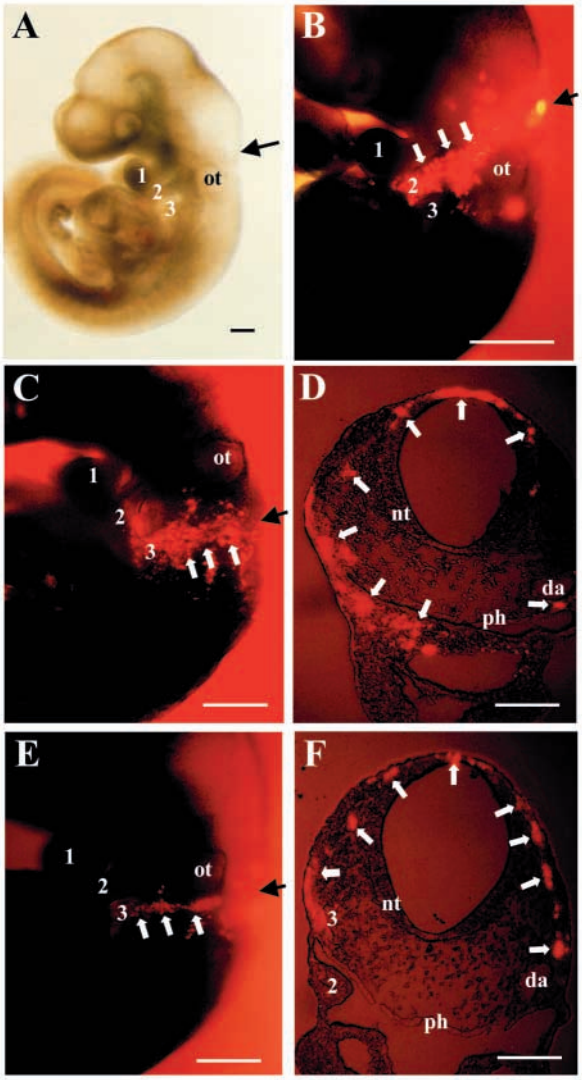

Fig. 2. Lateral views (A-C,E) and transverse sections (D,F) of ICR embryos after 48 hours in vitro. (A) An embryo which was injected with DiI at prorhombomere b (ProRhB) (arrow marks injection site) appears normal at 48 hours. (B) In this embryo, a stream of DiI-labelled cells (white arrows) is observed extending from the labelling site (black arrow) to the second pharyngeal arch (2). (C) Following injection of another embryo in prorhombomere c (ProRhC) (black arrow), DiI-labelled cells (white arrows) are seen extending into the third pharyngeal arch (3). (D) A section through the level of the labelling site in C shows DiI-labelled cells (white arrows) in a dorsolateral pathway that extends from the dorsal side of the neural tube to the level of the developing pharynx (ph). (E) Grafting of a DiI-labelled neural crest fragment into ProRhC (black arrow), produces a narrow stream of labelled cells (white arrows) passing from the graft site to the third pharyngeal arch (3). (F) A section through the graft site of the embryo in E shows a similar distribution of labelled cells (white arrows) as in the DiI-injected embryo (C,D). Scale bars: 160 μm in A-C,E; 80 μm in D,F. da, dorsal aorta; ot, otic vesicle; ph, pharynx.

levels S1, S2, S3 or S4, labelled cells were found in the third, fourth and sixth pharyngeal arches instead of being restricted to one single pharyngeal arch, suggesting a degree of rostrocaudal spreading of the neural crest entering the caudal

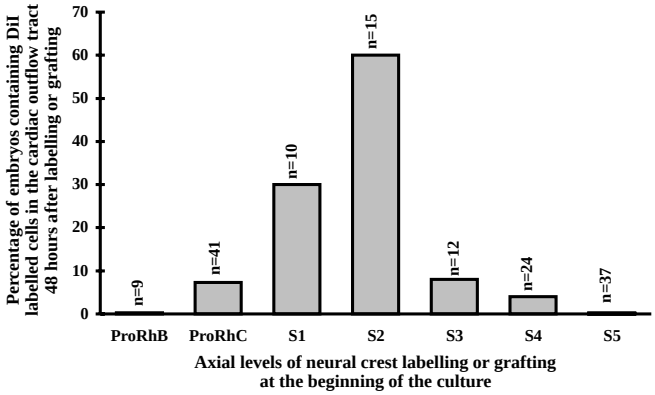

Fig. 3. Percentage of ICR embryos with DiI-labelled cells in the cardiac outflow tract 48 hours after injection with DiI or grafting with a DiI-labelled neural crest fragment at different axial levels of the neural crest. n, number of embryos analysed.

pharyngeal arches (Fig. 4A,B). Labelled cells were also located ventral to the pharynx and in the proximal end of the cardiac outflow tract (Fig. 3, Fig. 4C). Most of the embryos (60%) that were labelled or grafted at the S2 level contained labelled cells in the cardiac outflow tract, whereas only 30%, 8% and 4% of embryos initially labelled or grafted at S1, S3 and S4 had labelled cells in the outflow tract, respectively (Fig. 3). These results suggest that the mouse cardiac neural crest originates from the neural tube between the levels of ProRhC and S4, with S2 being the most prolific source of cardiac neural crest. Labelling or grafting the neural crest at S5 produced labelled cells in the developing foregut, but not in the cardiac outflow tract (Fig. 4D).

Migratory pathways of cardiac neural crest cells

Next, we mapped in greater detail the migratory pathways of neural crest cells from their site of origin, at the level of ProRhC to S4, to the cardiac outflow tract. Focal labelling (n=195) or orthotopic grafting of a labelled neural crest fragment (n=123) was performed using DiI or WGA-Au. Embryos were cultured for up to 48 hours and migratory pathways were reconstructed from images of serial transverse sections. The migratory pathways deduced from focal labelling closely resembled those found by orthotopic grafting, both in space and time, regardless of whether WGA-Au or DiI was used. More labelled cells were observed, however, following focal labelling than after orthotopic grafting (e.g. compare Fig. 5G and Fig. 5H).

At the mid-ProRhC level, labelled cells began to detach from the dorsal edge of the neural tube and migrate into the cranial mesenchyme at the 7-somite stage (n=6; Fig. 5A). The labelled cells migrated along a dorsolateral pathway, beneath the surface epithelium and lateral to the anterior cardinal vein, reaching the peri-aortic region by the 11-somite stage (n=5; Fig. 5C). In contrast, cells labelled at the level of S1, S2, S3 and S4 exhibited a more complex migratory pattern. The following description of neural crest migration from S1-S4 levels is based on embryos labelled at S2 (n=79). The migratory behaviour of neural crest at S1 (n=73), S3 (n=59) and S4 (n=51) levels was closely similar. Neural crest emigration from the dorsal neural tube was underway by the

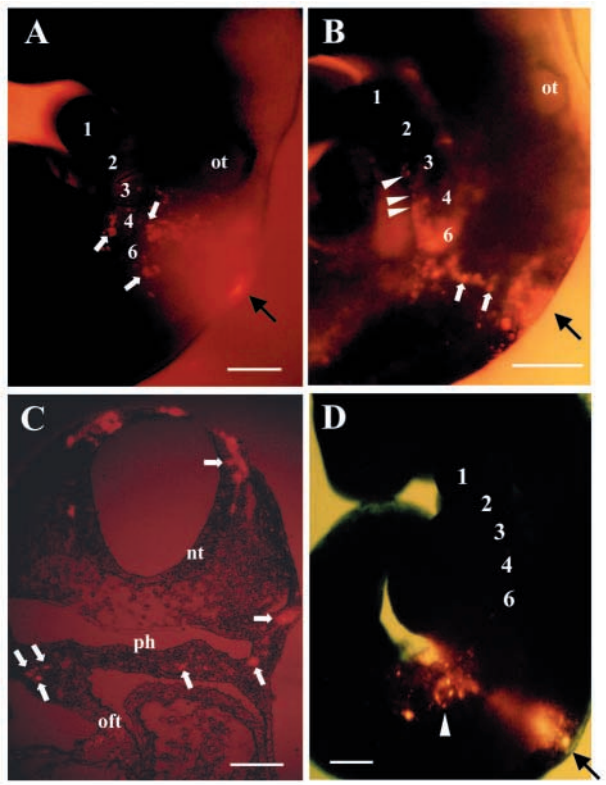

Fig. 4. Lateral views (A,B,D) and transverse section (C) of ICR embryos after 48 hours in vitro. (A,B) DiI-labelled cells (white arrows) are seen spreading from the labelling site (black arrow) to the third (3), fourth (4) and sixth (6) pharyngeal arches after injection at the level of the first somite (A), or after grafting with a DiI-labelled neural crest fragment at the level of the fourth somite (B). Some labelled cells are found in the aortic sac and cardiac outflow tract (oft) (arrowheads in B). (C) Section through the level of the graft site of the embryo in B confirms that some labelled cells (arrows) have reached the proximal end of the oft ventral to the pharynx (ph). (D) DiI injection of neural crest at the level of the fifth somite (black arrow) produces labelled cells in the foregut (arrowhead) but not in the pharyngeal arches nor any cardiac structures. Scale bars: 160 μm in A,B,D; 80 μm in C. nt, neural tube; ot: otic vesicle.

7-somite stage (*n*=19), with labelled cells having reached the region above the dorsal tip of the somite (Fig. 5B). At the 11-somite stage (*n*=6), labelled cells were visible along the dorsolateral pathway between the surface epithelium and the somite (Fig. 5D), along the medial pathway between the somite and the neural tube, where most labelled cells were found in the sclerotomal mesenchyme (Fig. 5D), and in an intersomitic pathway between successive somites (Fig. 5E). By 13-somites, early migrating neural crest had traversed ventrally to the peri-aortic region (*n*=8; Fig. 5F), presumably via the pathways observed at the previous stages, and, by 17 somites (*n*=12), many labelled cells were located dorsolateral or lateral to the developing pharynx (Fig. 5G). At this stage, labelled cells could still be seen in the medial pathway, whereas close apposition of the dermomyotome to the surface epithelium had largely obliterated the dorsolateral pathway.

At subsequent stages, further ventral migration through the pharyngeal arches appeared to slow down, whereas the third to sixth pharyngeal arches were undergoing expansion. Translocation of labelled cells became visible ventral to the pharynx at the 21-somite stage (*n*=22; Fig. 5H). Labelled neural crest cells continued to arise from the neural tube, at the level of ProRhC to S4, until the 23-somite stage (*n*=25), at which time the basal aspect of the dorsal neuroepithelium resumed a smooth contour and emigrating cells were no longer observed (Fig. 5I). At 26 somites (*n*=7), some of the most ventrally migrating neural crest cells reached the proximal end of the cardiac outflow tract (Fig. 6A), and by 32 somites (*n*=5) a few neural crest cells could be seen within the mesenchyme of the outflow tract (Fig. 6B).

Migratory pathways of splotch cardiac neural crest

Colonisation of the cardiac outflow tract by neural crest is defective in the *splotch* mutant (Conway et al., 1997; Conway et al., 2000; Henderson et al., 1997; Epstein et al., 2000). To study s*plotch* neural crest migration in detail, we focally labelled the cardiac neural crest with WGA-Au and cultured the labelled embryos for 0 to 24 hours. A total of 131 *splotch* embryos were cultured and their development in vitro was found to closely resemble embryos developing entirely in vivo (data not shown). For example, 70% (7/10) of cultured Sp^{2H}/Sp^{2H} mutant embryos exhibited a persistently open cranial neural tube (exencephaly) compared with 71% (5/7) of in vivo controls. In agreement with previous work (Conway et al., 1997), we found no obligatory relationship between neural crest migration and success or failure of cranial neural tube closure. Hence, homozygous *splotch* mutant embryos with an open cranial neural tube were included in the subsequent analysis of neural crest migration pathways.

Cardiac neural crest migration in *splotch* embryos at the level of S2 was compared with non-cardiac neural crest migration from the levels of ProRhA and ProRhB. The spatio-temporal distribution of labelled neural crest from ProRhA and ProRhB of wild type (+/+), heterozygous (Sp^{2H}/+) and homozygous (Sp^{2H}/Sp^{2H}) *splotch* embryos was found to be very similar to that observed in non-mutant ICR embryos (data not shown). At 9, 12-13, 16-17 and 20-21 somites, the numbers of labelled cells in the trigeminal ganglion, facio-acoustic ganglion and second pharyngeal arches were similar in ICR and in all three *splotch* genotypes (Fig. 7A-C). Hence, the *Pax3* mutation in *splotch* does not appear to have a major effect on the migration of neural crest cells at the level of the rostral hindbrain, consistent with previous findings (Serbedzija and McMahon, 1997).

At the S2 level, labelled neural crest cells began to emigrate from the dorsal part of the neural tube at the 7- to 8-somite stage in all wild-type (*n*=4) and heterozygous (*n*=8) embryos (Fig. 8A,B). In contrast, none of the 7- to 8-somite Sp^{2H}/Sp^{2H} homozygous embryos examined (*n*=5) showed labelled cells emigrating from the neural tube (Fig. 8C). At 9 somites, labelled cells were observed in the medial pathway in +/+ (*n*=6) and Sp^{2H}/+ (*n*=6) embryos, as in ICR embryos (*n*=5) (Fig. 7D). Labelled migrating cells were not observed, however, in the cranial mesenchyme of Sp^{2H}/Sp^{2H} embryos (*n*=6) at this stage (Fig. 7D), but only in embryos with more than 10 somites.

In embryos with 12 to 13 somites, labelled cells were observed in +/+ (*n*=9) and Sp^{2H}/+ (*n*=14) embryos along the dorsolateral, medial and intersomitic pathways, with the

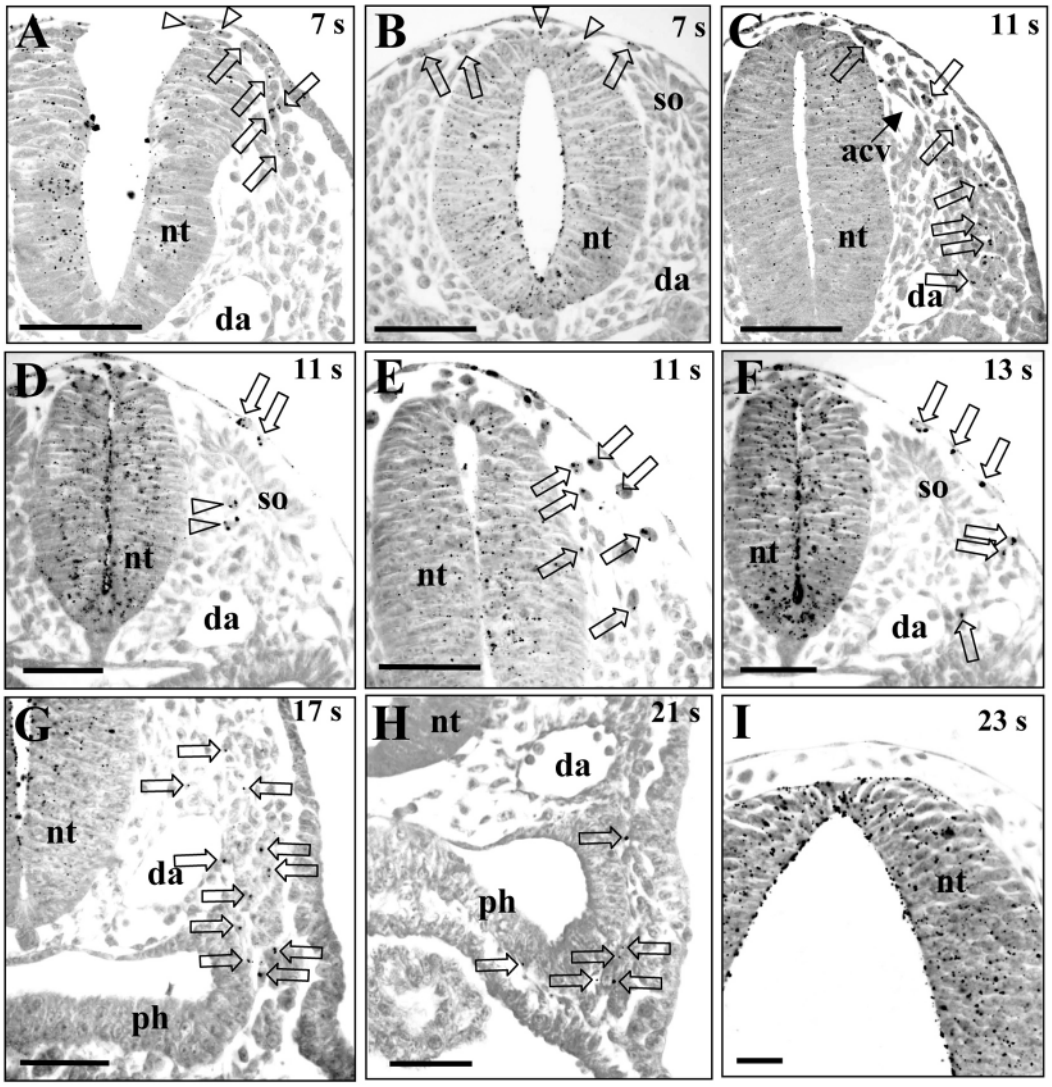

Fig. 5. Transverse sections of ICR embryos through mid-prorhombomere c (ProRhC) (A,C) or somite 2 (B,D-I). Embryos were fixed at different time points after labelling at the 5-6 somite stage by WGA-Au injection (A-G,I) or grafting of a WGA-Au-labelled neural crest fragment (H). At the 7-somite stage, WGA-Au-labelled cells, which carry dark silver granules (arrowheads in A,B), are seen leaving the dorsal part of the neural tube and some labelled cells are found in the mesenchyme beneath the surface epithelium (arrows in A) or at the dorsal tip of the somite (arrows in B; so, somite). At 11 somites after labelling at ProRhC (C), labelled cells (arrows in C) are located in the dorsolateral pathway beneath the surface epithelium and lateral to the anterior cardinal vein (acv in C). At the same stage after labelling at the somite-2 level (D,E), labelled cells (arrows in D) are observed in the dorsolateral pathway, between somite and surface epithelium, and also in the medial pathway (arrowheads in D) between neural tube (nt) and the somite (so). Another embryo shows WGA-Au-labelled neural crest cells in the intersomitic pathway (arrows in E). By the 13-somite stage, labelled cells (arrows in F) are more ventrally located, in the region adjacent to the dorsal aorta (da). At 17 somites (G), some labelled cells (arrows in G) have migrated beyond the somite to the region lateral to the developing pharynx (ph). By 21 somites, labelled cells (arrows in H) have reached the ventral side of the pharynx. Note that the spatio-temporal distribution of the labelled cells following grafting of a piece of neural crest tissue (H) is very similar to that observed after WGA-Au injection (G), although the number of labelled cells is smaller after grafting than labelling. At 23 somites (I), no more labelled cells are seen emigrating from the dorsal part of the nt, which exhibits a smooth contour on its basal surface. Scale bars: 50 μm in A-H; 20 μm in I.

earliest migrating cells having reached the peri-aortic mesenchyme by this stage (Fig. 8D,E). In contrast, in Sp^{2H}/Sp^{2H} embryos (n=15) labelled cells were not found in the dorsolateral pathway, but could be seen in the medial and intersomitic pathways. Their migration in the latter two pathways was retarded, however, with the most ventrally located labelled cells only having reached the ventral tip of the somite by the 12-13 somite stage (Fig. 8F). It was noticeable that the number of labelled neural crest cells in Sp^{2H}/Sp^{2H} embryos was significantly lower than in +/+ and Sp^{2H}/+ littermates at this stage (Fig. 7D,E).

At 16 to 17 somites, many labelled cells had migrated to the region lateral to the developing pharynx of +/+ (n=9) and Sp^{2H}/+ (n=12) embryos (Fig. 8G,H), whereas in Sp^{2H}/Sp^{2H} (n=11) embryos, significantly fewer labelled cells were present and these had only reached the peri-aortic mesenchyme (Fig. 7E, Fig. 8I). Labelled neural crest was not present in the mesenchyme lateral to the pharynx of Sp^{2H}/Sp^{2H} embryos at this stage (Fig. 7F, Fig. 8I). By 20 to 21 somites, labelled cells in both +/+ (n=5) and Sp^{2H}/+ (n=18) embryos had translocated ventral to the pharynx (Fig. 8J,K), whereas Sp^{2H}/Sp^{2H} embryos (n=8) exhibited fewer labelled cells and these were no farther ventral than the pharynx (Fig. 7F, Fig. 8L).

In conclusion, up to the 21-somite stage, significantly fewer labelled cells were observed in the medial pathway and peri-aortic mesenchyme of Sp^{2H}/Sp^{2H} embryos, compared with +/+ and Sp^{2H}/+ littermates, whereas *splotch* homozygotes showed no labelled neural crest ventral to the pharynx (Fig. 7D-F).

Interactions between the splotch neural crest and its migratory environment

To determine whether the retarded neural crest migration in

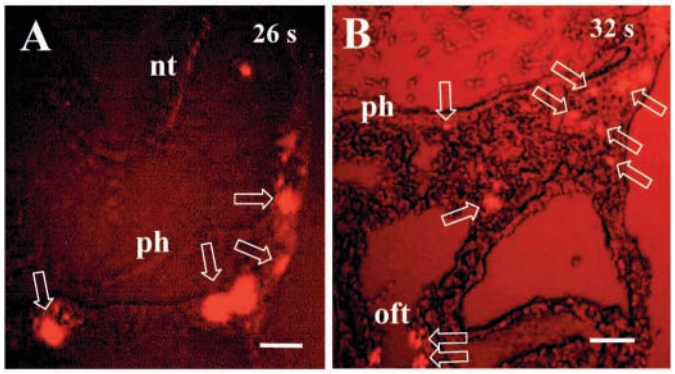

Fig. 6. Transverse sections through ICR embryos with 26 somites (A) and 32 somites (B) after labelling with DiI at the level of the second somite. The most ventrally located labelled cells (arrows) are in regions lateral and ventral to the pharynx (ph) at 26 somites, and by 32 somites, labelled cells have reached the wall of the cardiac outflow tract (oft). Scale bars: 40 μm in A; 20 μm in B. nt, neural tube.

splotch embryos is cell-autonomous or regulated by the migratory environment, we performed orthotopic grafting of WGA-Au-labelled neural crest fragments at the 5- to 6-somite stage between embryos of different *splotch* genotypes (Table 1). All grafts were performed without knowledge of the genotype combination which was revealed only retrospectively. A total of 135 *splotch* embryos were grafted, of which 103 (76%) had the graft successfully placed in the neural crest region, and were subsequently cultured. After 24 hours of culture, 12 embryos (12%) had failed to undergo axial rotation and were discarded. Of the 25 Sp^{2H}/Sp^{2H} recipient embryos, 16 (64%) exhibited an open cranial neural tube suggesting that grafting had not normalised cranial neural tube closure.

Neural crest fragments isolated from wild-type donor embryos were found to incorporate successfully into the dorsal part of the neural tube of wild type (+/+→+/+) (Fig. 9A), heterozygous (+/+→Sp^{2H}/+) and homozygous recipients (+/+→Sp^{2H}/Sp^{2H}). Moreover, labelled +/+ cells were found along the normal migratory pathways of the cardiac neural crest in these embryos (Fig. 9B, Table 1). Similarly, when either Sp^{2H}/+ or Sp^{2H}/Sp^{2H} embryos were used as neural crest donors, and grafted to a wild-type recipient embryo (i.e. Sp^{2H}/+→+/+ or Sp^{2H}/Sp^{2H}→+/+), the graft incorporated successfully (Fig. 9C) and the migratory behaviour of labelled graft-derived neural crest cells appeared normal (Fig. 9D, Table 1). Hence, presence of the *splotch* mutation in the graft alone, or in the migratory environment alone, was compatible with a normal pattern of neural crest migration. In contrast, when both donor and recipient embryos were of heterozygous or

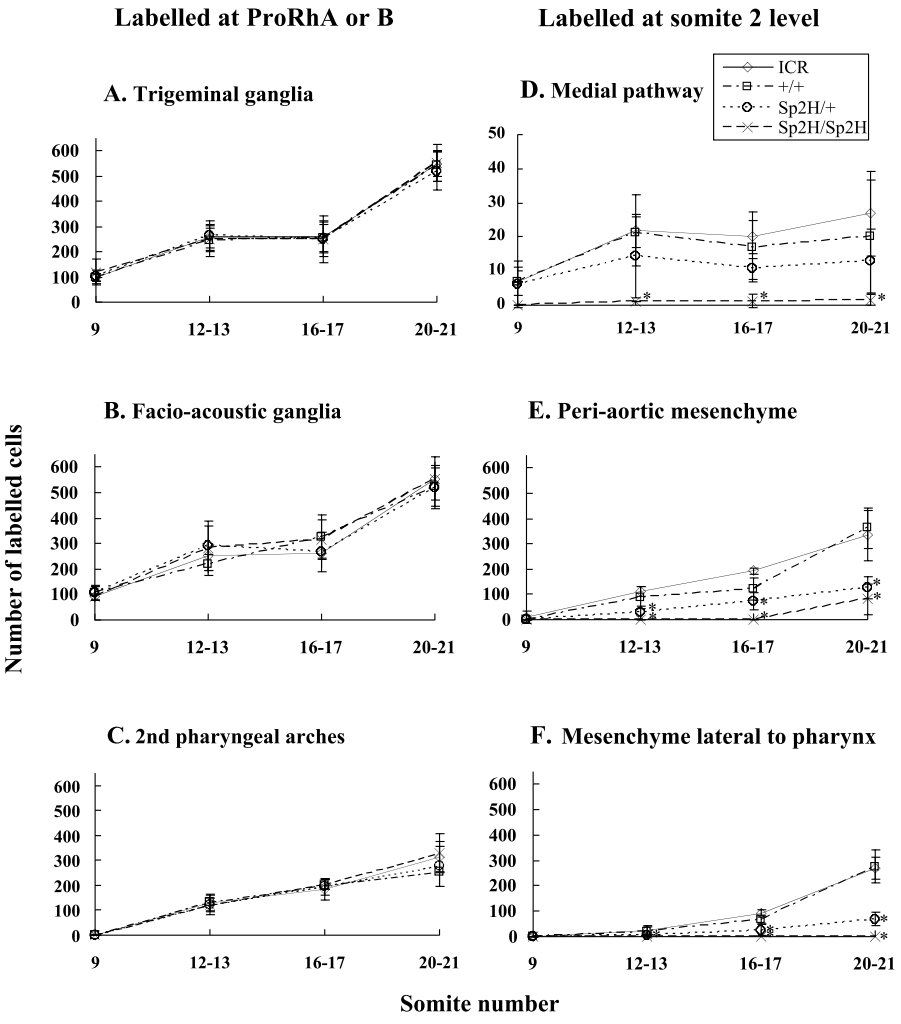

Fig. 7. Number of WGA-Au-labelled cells in different regions of ICR and s*plotch* mutant embryos at different somite stages following labelling of the neural crest in prorhombomere a (ProRhA) or prorhombomere b (ProRhB) (A-C) or at the level of the second somite (D-F). Note that the scale on the *y*-axis in D is different from other graphs. ICR embryos and wild type (+/+), heterozygous (Sp^{2H}/+) and homozygous (Sp^{2H}/Sp^{2H}) embryos from *splotch* litters all show similar numbers of labelled cells in the trigeminal ganglia (A), the facio-acoustic ganglia (B) and the second pharyngeal arches (C) at the 9-, 12-13, 16-17 and 20-21-somite stage, following labelling of neural crest at ProRhA or ProRhB. In contrast, labelling of the neural crest at the level of the second somite produced significantly fewer labelled cells in *splotch* mutants in the following regions: medial pathway (i.e. sclerotomal mesenchyme between the somite and the neural tube) of the homozygous (Sp^{2H}/Sp^{2H}) embryos with 9, 12-13, 16-17 and 20-21 somites (D); peri-aortic mesenchyme of heterozygous (Sp^{2H}/+) and homozygous (Sp^{2H}/Sp^{2H}) embryos with 12-13, 16-17 and 20-21 somites (E); and the mesenchymal region lateral to the developing pharynx of homozygous (Sp^{2H}/Sp^{2H}) embryos with 12-13 somites and heterozygous (Sp^{2H}/+) and homozygous (Sp^{2H}/Sp^{2H}) embryos with 16-17 and 20-21 somites (F). The number of labelled cells at each time point was computed from at least 5 embryos (bars: s.e.m.). *Significantly different from the value for ICR embryos with the same somite number by Student's two-tailed *t*-test ($P<0.05$).

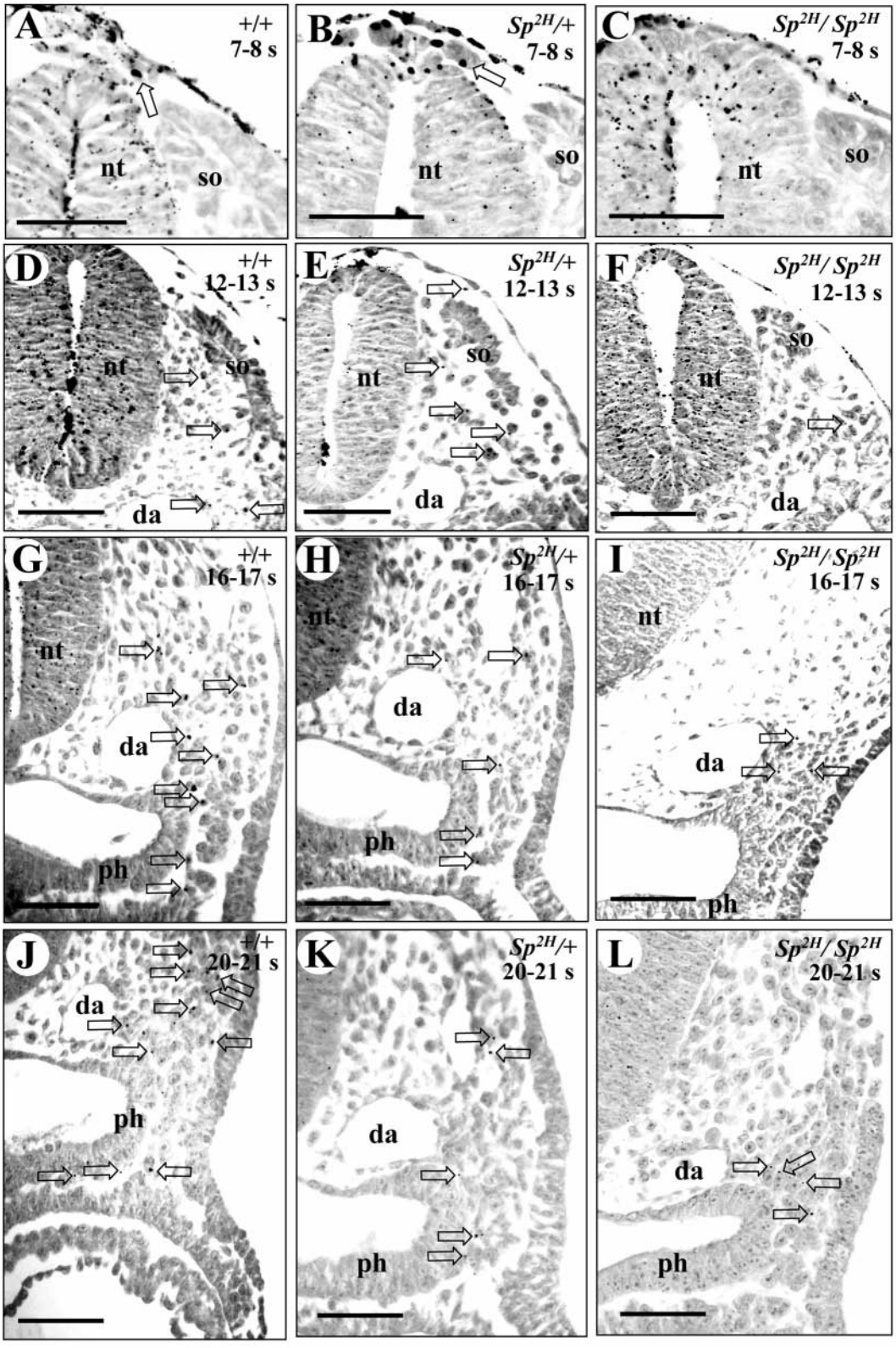

Fig. 8. Transverse sections through wild type (+/+) (A,D,G,J), heterozygous (Sp^{2H}/+) (B,E,H,K) and homozygous (Sp^{2H}/Sp^{2H}) (C,F,I,L) *splotch* embryos with 7-8 somites (A-C), 12-13 somites (D-F), 16-17 somites (G-I) and 20-21 somites (J-L) after labelling with WGA-Au at the level of the second somite. At 7-8 somites, labelled neural crest cells (arrows in A,B) are seen emigrating from the neural tube into the dorsal mesenchyme underneath the surface epithelium in both +/+ and Sp^{2H}/+ embryos. In contrast, Sp^{2H}/Sp^{2H} embryos do not show any labelled cells in the same mesenchymal region (C). At 12 to 13 somites (D,E), more labelled cells can be seen migrating in the dorsolateral and medial pathways (arrows in D,E) in +/+ (D) and Sp^{2H}/+ embryos (E). Some labelled cells have already reached the peri-aortic region. Sp^{2H}/Sp^{2H} embryos at the same stage (F) show fewer labelled cells in the cranial mesenchyme, which are mainly located dorsal to the dorsal aorta (arrow in F). At 16-17 somites, +/+ (G) and Sp^{2H}/+ (H) embryos contain labelled cells (arrows in G,H) that have passed beyond the dorsal aorta and are localised lateral to the developing pharynx. In contrast, labelled cells in Sp^{2H}/Sp^{2H} embryos (arrows in I) are now present in regions lateral to the dorsal aorta. By 20 to 21 somites, labelled cells have traversed to the ventral side of the pharynx in both +/+ (J) and Sp^{2H}/+ (K) embryos whereas, in Sp^{2H}/Sp^{2H} (L) embryos, labelled cells are located dorsolateral to the pharynx, but not at more ventral locations. Scale bar: 50 μm. da, dorsal aorta; nt, neural tube; ph, pharynx.

homozygous *splotch* mutant genotype, abnormal neural crest migration was observed (Fig. 9F,G), despite the successful incorporation of the graft into the dorsal neural tube (Fig. 9E,G). Sp^{2H}/+ grafts into Sp^{2H}/+ recipient embryos yielded a mostly normal pattern and frequency of neural crest migration, although only 50% of embryos showed labelled cells lateral to the pharynx (Table 1; not statistically significant). Sp^{2H}/+ grafts into Sp^{2H}/Sp^{2H} recipients, however, yielded a statistically significant reduction in neural crest migration, as did Sp^{2H}/Sp^{2H} grafts into Sp^{2H}/Sp^{2H} recipients (Fig. 9G).

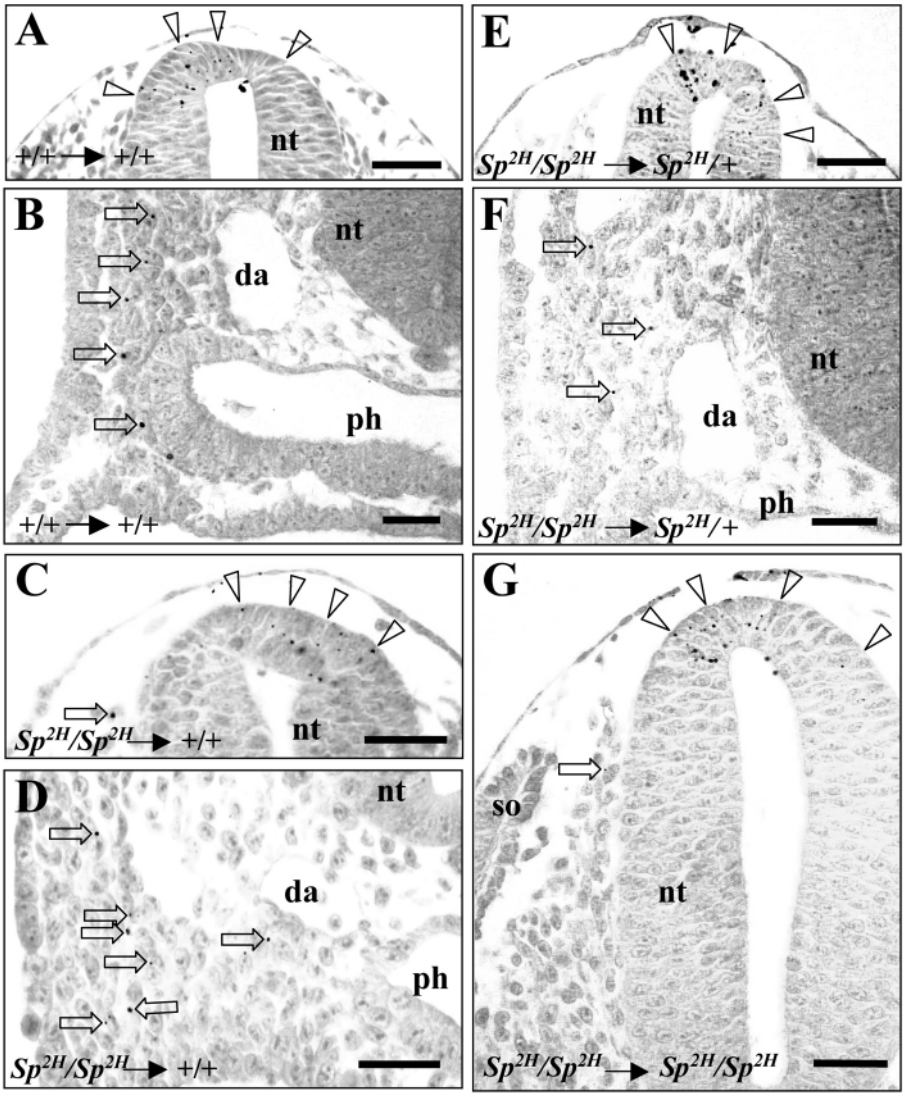

Fig. 9. Transverse sections through recipient embryos 24 hours after receiving an orthotopic WGA-Au-labelled neural crest graft at the level of the second somite. Graft combinations (donor→recipient) are: (A,B) +/+→+/+; (C,D) *Sp*^{2H}/*Sp*^{2H}→+/+; (E,F) *Sp*^{2H}/*Sp*^{2H} →*Sp*^{2H}/+; (G) *Sp*^{2H}/*Sp*^{2H}→*Sp*^{2H}/*Sp*^{2H}. Note that all grafts (outlined by arrowheads in A,C,E,G) successfully incorporated into the dorsal neural tube of recipient embryos. In the +/+→+/+ (B) and *Sp*^{2H}/*Sp*^{2H}→+/+ (D) embryos, labelled graft-derived cells (arrows) can be seen migrating lateral to the dorsal aorta (da), reaching as far ventrally as the pharynx (ph). In the *Sp*^{2H}/*Sp*^{2H}→*Sp*^{2H}/+ embryo (F), labelled cells (arrows) are migrating, but have not progressed beyond the dorsal aorta. Most strikingly, in the *Sp*^{2H}/*Sp*^{2H}→*Sp*^{2H}/*Sp*^{2H} embryo (G), only one labelled cell (arrow in G) has emerged from the graft, and has migrated only a short distance lateral to the neural tube (nt). Scale bars: 25 μm in A-C,E; 13 μm in D,F,G. da, dorsal aorta; nt, neural tube; ph, pharynx.

Interestingly, *Sp*^{2H}/*Sp*^{2H} neural crest grafted into a *Sp*^{2H}/+ recipient showed some degree of rescue, although there was a significant absence of neural crest reaching the pharynx (Fig. 9F, Table 1). These findings suggest that the abnormalities in migration of cardiac neural crest seen in *splotch* embryos require the genetic defect in both neural crest cells and their migratory environment.

Discussion

In the present study, three questions were investigated with regard to the migration of the mammalian cardiac neural crest, using the mouse embryo as an experimental model. In the following sections we discuss our findings and offer answers to our three original questions.

Axial level of origin of the mouse cardiac neural crest

In birds, the region of the neural crest contributing cells to the developing heart arises from the axial level between the midotic placode and the caudal limit of somite 3 (Kirby and Waldo, 1990; Kirby and Waldo, 1995; Miyagawa-Tomita et al., 1990). The neural crest from rhombomeres 6 to 8, which extend down as far as somite 4, has also been shown to contribute to the wall of the pharyngeal arch arteries and the aorto-pulmonary septum (Couly et al., 1998). In mammals, however, the rostrocaudal extent of the cardiac neural crest along the neural axis has not been clearly delineated. DiI labelling of the premigratory neural crest in rat embryos showed that cells from the level of the first to fourth occipital somites migrate to the cardiac outflow tract. Colonisation of cardiac structures by labelled cells was not observed when the neural crest was labelled just rostral to the first somite or just caudal to the fourth somite (Fukiishi and Morriss-Kay, 1992). The discrepancy in the apparent rostral extent of the cardiac neural crest in the chick and rat has been attributed to anatomical differences between the species: the region between the post-otic and pre-somitic hindbrain is longer in mammals than birds, whereas an additional pair of occipital somites is found in birds compared with mammals (Fukiishi and Morriss-Kay, 1992).

More recently, transgenic fate-mapping using Cre-loxP technology has provided information on the cardiac neural crest of the mouse. Cells expressing the *lacZ* reporter, expressed because of activation of the Wnt1 promoter in the premigratory neural crest, were detected in the developing pharyngeal arch arteries and the cardiac outflow tract with similar, although not identical, distribution patterns to those found in avian hearts (Jiang et al., 2000). These findings have confirmed the existence of a cardiac neural crest lineage in mammals (Lo et al., 1997; Yamauchi et al., 1999; Jiang et al., 2000; Li et al., 2000). However, because the transgenes are expressed in the neural crest at all axial levels (Jiang et al., 2000; Li et al., 1999; Lo et al., 1997; Pietri et al., 2003) or

Table 1. Distribution of WGA-Au-labelled cells in *splotch* embryos after orthotopic grafting*

Genotype of donor tissue	Genotype of recipient embryos	Number of recipients examined	Number of embryos (%) showing labelled cells along the migratory pathways: Mesenchymal region dorsolateral to the neural tube	Medial pathway	Peri-aortic mesenchyme	Mesenchymal region lateral to the pharynx
+/+	+/+	6	6 (100%)	6 (100%)	6 (100%)	6 (100%)
	Sp^{2H}/+	16	16 (100%)	16 (100%)	16 (100%)	16 (100%)
	Sp^{2H}/Sp^{2H}	7	7 (100%)	7 (100%)	7 (100%)	5 (71%)
Sp^{2H}/+	+/+	10	10 (100%)	8 (80%)	10 (100%)	8 (80%)
	Sp^{2H}/+	24	24 (100%)	16 (67%)	24 (100%)	12 (50%)
	Sp^{2H}/Sp^{2H}	10	2 (20%)†	2 (20%)†	2 (20%)†	1 (10%)†
Sp^{2H}/Sp^{2H}	+/+	7	7 (100%)	7 (100%)	7 (100%)	7 (100%)
	Sp^{2H}/+	3	3 (100%)	3 (100%)	3 (100%)	0†
	Sp^{2H}/Sp^{2H}	8	2 (25%)†	1 (13%)†	1 (13%)†	1 (13%)†

**Splotch* embryos with 5 to 6 somites were orthotopically grafted with a WGA-Au-labelled neural crest fragment at the S2 level and were cultured in vitro for 24 hours. Embryos with 20 to 21 somites were examined for the distribution of labelled cells after sectioning.

†$P<0.05$, significantly different from the value for +/+ → +/+ grafting by Fisher's exact test.

expressed only at relatively advanced stages when the neural crest cells have already come close to the heart (Tremblay et al., 1995), it is difficult from these studies to ascertain the axial levels of origin of the cardiac neural crest.

In the present study, we performed a rostrocaudal, region-by-region analysis of neural crest migratory fate, and found that the mouse cardiac neural crest arises from a length of neural tube extending from the post-otic hindbrain to the caudal limit of somite 4. This observation agrees with previous findings in the chick. We demonstrated, moreover, that the neural tube at the level of somite 2 is quantitatively the most prolific source of cardiac neural crest. Cells arising from ProRhC (the post-otic region rostral to the first somite) (Osumi-Yamashita et al., 1996), and from the neural tube at the level of somites 3 and 4, contribute fewer cells to the developing outflow tract. This finding suggests that the mouse neural crest has rather specific migratory fates, depending on its precise axial level of origin, and that there is unlikely to be much mixing between neural crest populations emanating from adjacent levels of the neural tube. This is in contrast to the chick where the pharyngeal arches 3 to 6 receive neural crest cells from a region of neural tube up to three somites in length (Shigetani et al., 1995).

Migratory pathways taken by cardiac neural crest in the mouse

Our study shows that the mouse cardiac neural crest emigrates from the neural tube between the 7- and 23-somite stages. In a similar way to the cranial neural crest (Le Douarin and Kalcheim, 1999; Chan and Tam, 1988), cardiac neural crest cells derived from the post-otic, pre-somitic ProRhC level were restricted to the dorsolateral pathway beneath the surface epithelium and lateral to the cardinal vein. In contrast, neural crest emanating from the levels of somites 1 to 4 exhibited a much more complex migration pattern, following dorsolateral, medial and intersomitic pathways, as previously described for the avian cardiac neural crest and for the trunk neural crest of both birds and mammals (for a review, see Le Douarin and Kalcheim, 1999). In birds, the early migrating cardiac crest occupies the dorsolateral pathway prior to colonisation of the medial pathways (Tucker et al., 1986; Kuratani and Kirby, 1991; Reedy et al., 1998), whereas we found mouse cardiac neural crest cells migrating simultaneously along all three pathways, similar to that described for early mouse trunk neural crest migration (Serbedzija et al., 1990). Spatially, the chick and mouse pathways also differ with the chick cardiac neural crest traversing the dorsolateral pathway at the levels from the somites 1 to somite 4 as in the mouse, but occupying the medial and intersomitic pathways only in regions caudal to somite 2 (Kuratani and Kirby 1991). Moreover, the chick medial pathway can be subdivided into ventrolateral (sclerotomal) and ventromedial (adjacent to the neural tube) components, whereas this subdivision was not distinct in the mouse.

The chick neural crest, migrating on the dorsolateral pathway, temporarily ceases its migration and forms a distinct longitudinal mass of cells within the lateral body wall, dorsolateral to the dorsal edge of the pericardium (Kuratani and Kirby, 1991; Kuratani and Kirby, 1992). This 'circumpharyngeal crest' subsequently populates the expanding pharyngeal arches. In the mouse, we did not observe the precocious arrival of neural crest prior to the lateral expansion of the caudal pharyngeal arches, and no distinct mass of 'circumpharyngeal crest' cells was observed within the lateral body wall.

Migration of cardiac neural crest in the splotch mutant mouse

Splotch is a well-recognized genetic model of neural crest and neural tube defects (Auerbach, 1954). Homozygous loss of *Pax3* function in *splotch* mice (Epstein et al., 1991; Epstein et al., 1993; Goulding et al., 1993; Vogan et al., 1993) produces a phenotype closely resembling that of chick embryos following cardiac neural crest ablation. This has led to the idea that cardiac neural crest development is compromised in *splotch* (Epstein, 1996; Conway et al., 1997).

Several lines of evidence support defective migration of neural crest cells from the neural tube to the heart in *splotch* embryos. Use of a Wnt-1::*lacZ* transgenic reporter revealed a severe reduction in the number of neural crest cells emigrating from both vagal and rostral trunk levels of the *splotch* neural tube (Serbedzija and McMahon, 1997). Moreover, a reduced number of migrating *splotch* neural crest cells has been deduced indirectly from the observation of decreased

expression of various neural crest markers and transgenes (Conway et al., 1997; Conway et al., 2000; Tremblay et al., 1995; Serbedzija and McMahon, 1997; Epstein et al., 2000). Alternatively, the *Cx43-lacZ* transgene is reported to be expressed similarly in the cardiac neural crest of wild type and *splotch* embryos. This has prompted the conclusion that *Pax3* is not essential for early cardiac neural crest migration but, rather, is important for fine-tuning the migratory behaviour of the cardiac neural crest cells upon their arrival in the heart (Esptein et al., 2000). Our findings do not support this latter conclusion, but instead confirm a reduction in the cardiac neural crest population of *splotch* embryos during the migratory phase towards the heart. We detected a delay by 3 somite stages (i.e. approximately 6 hours of development) in the onset of cardiac neural crest emigration from the *splotch* homozygous neural tube. This early, transient delay in the onset of neural crest emigration can explain why *splotch* embryos at more advanced stages have been reported to exhibit normal neural crest emigration (Conway et al., 1997; Conway et al., 2000). Moreover, our direct labelling of the premigratory neural crest shows that although mutant neural crest cells are capable of migrating along normal pathways, the number of the cells en route is significantly reduced in *splotch* homozygotes, with a discernible reduction also in heterozygotes. Hence, our studies support the suggestion that a decrease in the number of migrating neural crest cells is the primary defect that ultimately leads to a lack of cardiac neural crest-derived cells in the outflow tract of *splotch* embryos (Conway et al., 2000).

We observed a reduced number of migrating neural crest cells only in the cardiac neural crest population of *splotch* embryos. Neural crest cells arising rostral to the otic vesicle appeared in normal numbers, with normal colonisation of cranial ganglia. Hence, there is an increase in the severity of the neural crest defect along the rostrocaudal axis of *splotch* embryos, consistent with previous findings (Auerbach, 1954; Serbedzija and McMahon, 1997).

Cell autonomy versus non-cell autonomy in splotch cardiac neural crest defects

An issue of some controversy is whether the defect of cardiac neural crest migration in *splotch* embryos is autonomous to the neural crest cell lineage, or whether it reflects an influence of the mutant migratory environment (non-cell autonomous). Transgenic reconstitution of *Pax3* expression solely in the dorsal neural tube (including the neural crest lineage) was reported to rescue neural tube closure, cardiac septation and dorsal root ganglion formation in *splotch* embryos (Li et al., 1999). This finding has been taken as strong evidence for a cell autonomous role of *Pax3* in the neural crest, although the study did not reveal whether the rescuing transgene was expressed in early cranial or paraxial mesoderm, tissues that provide the immediate migratory environment for the emigrating neural crest. Several other lines of evidence support a different view of the *splotch* neural crest defect. Neural crest cells derived from the caudal trunk level (Serbedzija and McMahon, 1997) or vagal level (Conway et al., 2000) of *splotch* embryos can follow normal migratory pathways after transplantation to chick embryos, suggesting that the migratory environment plays a crucial role in regulating neural crest migration. Similarly, chimaera studies, in which wild type and *Pax3*-deficient cells co-exist in the same embryo (Mansouri et al., 2001), have supported a non-cell autonomous mechanism for the *splotch* neural crest defect. Abnormalities of extracellular matrix composition in early *splotch* embryos are consistent with an adverse effect of the migratory environment on the neural crest (Henderson et al., 1997).

Our results offer a possible resolution of this controversy. We transplanted labelled premigratory neural crest cells between *splotch* embryos of different genotypes and found that the defects of cardiac neural crest migration occurred only when both donor and recipient embryos were of mutant genotype. Having either a wild-type neural crest lineage, or a wild-type migratory environment, was sufficient to rescue neural crest migration. Alternatively, even a *splotch* heterozygous neural crest lineage performed poorly in a homozygous mutant environment. Interestingly, the reverse was less true. Homozygous *splotch* neural crest cells migrated more effectively in a heterozygous environment. We conclude that the *splotch* mutant effect is mediated both through the neural crest cell lineage and the migratory environment, but that the effect of the environment may be more potent.

There is much evidence to support a critical role for reciprocal interactions between neural crest and environment in regulating migration (for a review, see Le Dourain and Kalcheim, 1999). The molecular composition of the neural crest cell surface, and of the migratory pathways, are both highly heterogeneous as well as temporally dynamic (Le Douarin and Kalcheim, 1999; Garcia-Castro and Bronner-Fraser, 1999; Christiansen et al., 2000; Maschhoff and Baldwin et al., 2000; Perris and Perissinotto, 2000). Different neural crest sub-populations, often varying in developmental potential, respond differently to a given migratory cue and continuously modify their fates during migration (Weston, 1991; Vaglia and Hall, 1999; White et al., 2001). Conversely, migrating neural crest cells also actively participate in shaping the molecular composition of their own migratory routes. It has been suggested that *Pax3* expression may be required to regulate cell surface properties (Mansouri et al., 2001), both on neural crest and its migratory environment, perhaps via downstream regulation of *Msx2* (Kwang et al., 2002). It remains to be determined precisely how this molecular pathway may enhance neural crest migration, and how its genetic disruption leads to defects of the cardiac neural crest.

The authors thank Alan J. Burns for his critical comments. This work was supported by the Research Grants Council of the Hong Kong Special Administrative Region, China (Project Nos. CUHK 4275/99M and CUHK4016/01M), and by the British Heart Foundation and the Wellcome Trust, UK (A.J.C.).

References

Auerbach, R. (1954). Analysis of the developmental effects of a lethal mutation in the house mouse. *J. Exp. Zool.* **127**, 305-329.

Brannan, C. I., Persins, A. S., Vogel, K. S., Ratner, N., Nordlund, M. L., Reid, S. W., Buchberg, A. M., Jenkins, N. A., Parada, L. F. and Copeland, N. G. (1994). Targeted disruption of the neurofibromatosis type-1 gene leads to developmental abnormalities of the heart and various neural crest-derived tissues. *Genes. Dev.* **8**, 1019-1029.

Chan, W. Y. and Lee, K. K. (1992). The incorporation and dispersion of latex beads on microinjection into the amniotic cavity of the mouse embryo at the early somite stage. *Anat. Embryol.* **185**, 225-238.

Chan, W. Y. and Tam, P. P. L. (1988). A morphological and experimental study of the mesencephalic neural crest cells in the mouse embryo using wheat germ agglutinin-gold conjugate as the cell marker. *Development* **102**, 427-442.

Chan, W. Y., Tam, W. Y., Yung, K. M., Cheung, C. S., Sham, M. H. and Copp, A. J. (2003). Tracking down the migration of mouse neural crest cells. *Neuroembryology* **2**, 9-17.

Christiansen, J. H., Coles, E. G. and Wilkinson, D. G. (2000). Molecular control of neural crest formation, migration and differentiation. *Curr. Opin. Cell Biol.* **12**, 719-724.

Conway, S. J., Bundy, J., Chen, J., Dickman, E., Rogers, R. and Will, B. M. (2000). Decreased neural crest stem cell expansion is responsible for the conotruncal heart defects within the *Splotch* (*Sp^{2H}*)/*Pax3* mouse mutant. *Cardiovasc. Res.* **47**, 314-328.

Conway, S. J., Henderson, D. J. and Copp, A. J. (1997). Pax3 is required for cardiac neural crest migration in the mouse: evidence from the *splotch* (*Sp^{2H}*) mutant. *Development* **124**, 505-514.

Couly, G., Grapin-Botton, A., Coltey, P., Ruhin, B. and Le Douarin, N. M. (1998). Determination of the identity of the derivatives of the cephalic neural crest: incompatibility between Hox gene expression and lower jaw development. *Development* **125**, 3445-3459.

Driscoll, D. A. (1994). Genetic basis of DiGeorge and velocardiofacial syndromes. *Curr. Opin. Pediatr.* **6**, 702-706.

Epstein, D. J., Vekemans, M. and Gros, P. (1991). *Splotch* (*Sp^{2H}*), a mutation affecting development of the mouse neural tube, shows a deletion within the paired homeodomain of Pax-3. *Cell* **67**, 767-774.

Epstein, D. J., Vogan, K. J., Trasler, D. G. and Gros, P. (1993). A mutation within intron 3 of the Pax-3 gene produces aberrantly spliced mRNA transcripts in the *splotch* (*Sp*) mouse mutant. *Proc. Natl. Acad. Sci. USA* **90**, 532-536.

Epstein, J. (1996). Pax3, neural crest and cardiovascular development. *Trends Cardiovasc. Med.* **6**, 255-261.

Epstein, J. A., Li, J., Lang, D., Chen, F., Brown, C. B., Jin, F., Lu, M. M., Thomas, M., Liu, E. J., Wessels, A. et al. (2000). Migration of cardiac neural crest cells in *Splotch* embryos. *Development* **127**, 1869-1878.

Franz, T. (1989). Persistent truncus arteriosus in the *Splotch* mutant mouse. *Anat. Embryol.* **180**, 457-464.

Fukiishi, Y. and Morriss-Kay, G. M. (1992). Migration of cranial neural crest cells to the pharyngeal arches and heart in rat embryos. *Cell Tissue Res.* **268**, 1-8.

Garcia-Castro, M. G. and Bronner-Fraser, M. B. (1999). Induction and differentiation of the neural crest. *Curr. Opin. Cell Biol.* **11**, 695-698.

Goulding, M., Sterrer, S., Fleming, J., Balling, R., Nadeau, J., Moore, K. J., Brown, S. D. M., Steel, K. P. and Gruss, P. (1993). Analysis of the *Pax-3* gene in the mouse mutant *Splotch*. *Genomics* **17**, 355-363.

Henderson, D. J., Ybot-Gonzalez, P. and Copp, A. J. (1997). Over-expression of the chondroitin sulphate proteoglycan *versican* is associated with defective neural crest migration in the *Pax3* mutant mouse (*Splotch*). *Mech. Dev.* **69**, 39-51.

Jiang, X., Rowitch, D. H., Soriano, P., McMahon, A. P. and Sucov, H. M. (2000). Fate of the mammalian cardiac neural crest. *Development* **127**, 1607-1616.

Kirby, M. L. and Stewart, D. E. (1983). Neural crest origin of cardiac ganglion cells in the chick embryo: identification and extirpation. *Dev. Biol.* **97**, 433-443.

Kirby, M. L. and Waldo, K. L. (1990). Role of neural crest in congenital heart disease. *Circulation* **82**, 332-340.

Kirby, M. L. and Waldo, K. L. (1995). Neural crest and cardiovascular patterning. *Circ. Res.* **77**, 211-215.

Kirby, M. L., Gale, T. F. and Stewart, D. E. (1983). Neural crest cells contribute to normal aorticopulmonary septation. *Science* **220**, 1059-1061.

Kuratani, S. C. and Kirby, M. L. (1991). Initial migration and distribution of the cardiac neural crest in the avian embryo: an introduction to the concept of the circumpharyngeal crest. *Am. J. Anat.* **191**, 215-227.

Kuratani, S. C. and Kirby, M. L. (1992). Migration and distribution of circumpharyngeal crest cells in the chick embryo. *Anat. Rec.* **234**, 263-280.

Kwang, S. J., Brugger, S. M., Lazik, A., Merrill, A. E., Wu, L. Y., Liu, Y. H., Ishii, M., Sangiorgi, F. O., Rauchman, M., Sucov, H. M. et al. (2002). *Msx2* is an immediate downstream effector of *Pax3* in the development of the murine cardiac neural crest. *Development* **129**, 527-538.

Le Douarin, N. M. and Kalcheim, C. (1999). *The Neural Crest*. Cambridge, UK: Cambridge University Press.

Li, J., Liu, K. C., Jin, F., Lu, M. M. and Epstein, J. A. (1999). Transgenic rescue of congenital heart disease and spina bifida in *Splotch* mice. *Development* **126**, 2495-2503.

Li, J., Chen, F. and Epstein, J. A. (2000). Neural crest expression of Cre recombinase directed by the proximal Pax3 promoter in transgenic mice. *Genesis* **26**, 162-164.

Lipson, A. H., Yuille, D., Angel, M., Thompson, P. B., Vandervoord, J. G. and Beckenham, E. J. (1991). Velo-cardio-facial (Shprintzen) syndrome: an important syndrome for the dysmorphologist to recognize. *J. Med. Genet.* **28**, 596-604.

Liu, Y. H., Ma, L., Wu, L. Y., Luo, W., Kundu, R., Sangiorgi, F., Snead, M. L. and Maxson, R. (1994). Regulation of the Msx2 homeobox gene during mouse embryogenesis: a transgene with 439 bp of 5′ flanking sequence is expressed exclusively in the apical ectodermal ridge of the developing limb. *Mech. Dev.* **48**, 187-197.

Lo, C. W., Cohen, M. F., Huang, G. Y., Lazatin, B. O., Patel, N., Sullivan, R., Pauken, C. and Park, S. M. (1997). Cx43 gap junction gene expression and gap junctional communication in mouse neural crest cells. *Dev. Genet.* **20**, 119-132.

Lo, C. W., Waldo, K. L. and Kirby, M. L. (1999). Gap junction communication and the modulation of cardiac neural crest cells. *Trends Cardiovasc. Med.* **9**, 63-69.

Lumsden, A., Sprawson, N. and Graham, A. (1991). Segmental origin and migration of neural crest cells in the hindbrain region of the chick embryo. *Development* **113**, 1281-1291.

Mansouri, A., Pla, P., Larue, L. and Gruss, P. (2001). *Pax3* acts cell autonomously in the neural tube and somites by controlling cell surface properties. *Development* **128**, 1995-2005.

Maschhoff, K. and Baldwin, H. S. (2000). Molecular determinants of neural crest migration. *Am. J. Med. Genet.* **97**, 280-288.

Means, A. L. and Gudas, L. J. (1997). The CRABP I gene contains two separable, redundant regulatory regions active in neural tissues in transgenic mouse embryos. *Dev. Dyn.* **209**, 59-69.

Miyagawa-Tomita, S., Waldo, K., Tomita, H. and Kirby, M. L. (1990). Migration of cardiac neural crest cells. *Ann. New York Acad. Sci.* **588**, 427-429.

Osumi-Yamashita, N., Ninomiya, Y., Doi, H. and Eto, K. (1996). Rhombomere formation and hind-brain crest cell migration from prorhombomeric origins in mouse embryos. *Dev. Growth Differ.* **38**, 107-118.

Perris, R. and Perissinotto, D. (2000). Role of the extracellular matrix during neural crest migration. *Mech. Dev.* **95**, 3-21.

Pietri, T., Eder, O., Blanche, M., Thiery, J. P. and Dufour, S. (2003). The human tissue plasminogen activator-Cre mouse: a new tool for targeting specifically neural crest cells and their derivatives in vivo. *Dev. Biol.* **259**, 176-187.

Reedy, M. V., Faraco, C. D. and Erickson, C. A. (1998). Specification and migration of melanoblasts at the vagal level and in hyperpigmented Silkie chickens. *Dev. Dyn.* **213**, 476-485.

Rothman, K. J., Moore, L. L., Singer, M. R., Nguyen, U. S., Mannino, S. and Milunsky, A. (1995). Teratogenicity of high vitamin A intake. *New Engl. J. Med.* **333**, 1369-1373.

Serbedzija, G. N. and McMahon, A. P. (1997). Analysis of neural crest cell migration in *Splotch* mice using a neural crest-specific lacZ reporter. *Dev. Biol.* **185**, 139-147.

Serbedzija, G. N., Bronner-Fraser, M. and Fraser, S. E. (1992). Vital dye analysis of the timing and pathways of avian trunk neural crest cell migration. *Development* **106**, 809-816.

Serbedzija, G. N., Fraser, S. E. and Bronner-Faser, M. (1990). Pathways of trunk neural crest cell migration in the mouse embryo as revealed by vital dye labelling. *Development* **108**, 605-612.

Shigetani, Y., Aizawa, S. and Kutatani, S. (1995). Overlapping origins of pharyngeal arch crest cells on the postotic hind-brain. *Dev. Growth Differ.* **37**, 733-746.

Smits-van Prooije, A. E., Poelmann, R. E., Dubbeldam, J. A., Mentink, M. M. and Vermeij-Keers, C. (1986). Wheat germ agglutinin-gold as a novel marker for mesectoderm formation in mouse embryos cultured in vitro. *Stain. Technol.* **61**, 97-106.

Trainor, P. A. and Tam, P. P. L. (1995). Cranial paraxial mesoderm and neural crest cells of the mouse embryo: co-distribution in the craniofacial mesenchyme but distinct segregation in branchial arches. *Development* **121**, 2569-2582.

Tremblay, P., Kessel, M. and Gruss, P. (1995). A transgenic neuroanatomical marker identifies cranial neural crest deficiencies associated with the *Pax3* mutant *Splotch*. *Dev. Biol.* **171**, 317-329.

Tucker, G. C., Ciment, G. and Thiery, J. P. (1986). Pathways of avian neural crest cell migration in the developing gut. *Dev. Biol.* **116**, 439-450.

Vaglia, J. L. and Hall, B. K. (1999). Regulation of neural crest cell populations: occurrence, distribution and underlying mechanisms. *Int. J. Dev. Biol.* **43**, 95-110.

Verberne, M. E., Gittenberger-de Groot, A. C. and Poelmann, R. E. (1998). Lineage and development of the parasympathetic nervous system of the embryonic chick heart. *Anat. Embryol.* **198**, 171-184.

Vogan, K. J., Epstein, D. J., Trasler, D. G. and Gros, P. (1993). The *Splotch-delayed* (*Spd*) mouse mutant carries a point mutation within the paired box of the *Pax-3* gene. *Genomics* **17**, 364-369.

Weston, J. A. (1991). Sequential segregation and fate of developmentally restricted intermediate cell populations in the neural crest lineage. *Curr. Top. Dev. Biol.* **149**, 133-153.

White, P. M., Morrison, S. J., Orimoto, K., Kubu, C. J., Verdi, J. M. and Anderson, D. J. (2001). Neural crest stem cells undergo cell-intrinsic developmental changes in sensitivity to instructive differentiation signals. *Neuron* **29**, 57-71.

Whittingham, D. G. and Wales, R. G. (1969). Storage of 2-cell mouse embryos in vitro. *Aust. J. Biol. Sci.* **22**, 1065-1068.

Winnier, G. E., Kume, T., Deng, K., Rogers, R., Bundy, J., Raines, C., Walter, M. A., Hogan, B. L. and Conway, S. J. (1999). Roles for the winged helix transcription factors MF1 and MFH1 in cardiovascular development revealed by nonalleic noncomplementation of null alleles. *Dev. Biol.* **213**, 418-431.

Yamauchi, Y., Abe, K., Mantani, A., Hitoshi, Y., Suzuki, M., Osuzu, F., Kuratani, S. and Yamamura, K. (1999). A novel transgenic technique that allows specific marking of the neural crest cell lineage in mice. *Dev. Biol.* **212**, 191-203.

Yanagisawa, H., Hammer, R. E., Richardson, J. A., Williams, S. C., Clouthier, D. E. and Yanagisawa, M. (1998). Role of Endothelin-1/Endothelin-A receptor-mediated signaling pathway in the aortic arch patterning in mice. *J. Clin. Invest.* **102**, 22-33.